Heat-induced self-assembling of BSA at the isoelectric point

*Lucia Comez[1], Pier Luigi Gentili[2], Marco Paolantoni[2], Alessandro Paciaroni[3] and Paola Sassi[*2,4]*

1: IOM-CNR c/o Dipartimento di Fisica e Geologia, Università di Perugia,

Via Pascoli, I-06123 Perugia, Italy

2: Dipartimento di Chimica, Biologia e Biotecnologie, Università degli Studi di Perugia,

Via Elce di sotto 8, 06123 Perugia

3: Dipartimento di Fisica e Geologia, Università di Perugia, Via Pascoli, I-06123 Perugia, Italy

4: Centro di Eccellenza sui Materiali Innovativi Nanostrutturati (CEMIN), Università di Perugia,

Via Elce di Sotto 8, 06123 Perugia, Italy

Abstract

Materials based on ordered protein aggregates have recently received a lot of attention for their application as drug carriers, due to their biocompatibility and their ability to sequester many biological fluids. Bovine serum albumin (BSA) is a good candidate for this use due to its high availability and tendency to aggregate and gel under acidic conditions. In the present work, we employ spectroscopic techniques to investigate the heat-induced BSA aggregation at the molecular scale, in the 12-84°C temperature range, at pH=5 where two different isoforms of the protein are stable. Samples at low and high protein concentration are examined. With the advantage of the combined use of FTIR and CD, we recognize the aggregation-prone species and the different distribution of secondary structures, conformational rearrangements and types of aggregates, of millimolar compared to micromolar BSA solutions. Further, as a new tool, we use the Maximum Entropy Method to fit the kinetic curves to investigate the distribution of kinetic constants of the complex hierarchical aggregation process. Finally, we characterize the activation energy of the initial self-assembling step to observe that the formation of both small and large aggregates is driven by the same interactions.

keywords: BSA, aggregation, spectroscopy, Maximum Entropy Method

This research did not receive any specific grant from funding agencies in the public, commercial, or not-for-profit sectors.

corresponding author

*e-mail: paola.sassi@unipg.it. Tel: +39 075 5855585. Fax: +39 075 5855586

Introduction

Serum albumin is a transport protein of the blood, the most abundant serum protein in mammals (50 mg/ml ca.). Due to its availability and stability, it is one of the most used model proteins in biophysical studies, both in the animal and human variants. Its structure is highly flexible and depends on the solvation conditions. At neutral pH, a negative net charge is distributed over a typical heart-shaped structure, having a 70% α-helical conformation, and divided into the three different homologous domains I, II, and III [1,2]. It is known that the soft BSA molecule undergoes multi-stage transformations and that the transformations are complex since all the three domains of the protein can rearrange independently [3]. They can be observed and characterized by thermal treatments or pH changes[4–9]. On increasing pH at room temperature, reversible transformations have been identified among five isomeric forms of BSA,[10] from the expanded (E), fast (F), normal (N), basic (B), and aged (A) forms. The F to E transition is assigned to the unfolding of the helical structure of the domain I. The N to F transition is assigned to the unfolding of the domain III; in this conformational change, the protein transits through its isoelectric point and reaches a +100 net charge at pH=3.5.

In a recent work, Baler et al.[11] give a detailed description of the charge distribution in BSA, allowing to recognize hydrophilic and hydrophobic regions of the molecule which strongly contribute to defining protein-solvent and protein-protein interactions. Concerning self-aggregation, they observe that this is particularly favored when the protein is in the F form due to the exposure of the hydrophobic groups to the solvent. Because of its open structure, the high positive surface charge is neutralized by counter-ions which are present in the solvation environment; this makes the hydrophobic interactions prevail and eventually lead to the formation of hydrogels.

The study of the aggregation properties of globular proteins is of great interest both in the biological field and in materials science. The formation of highly ordered aggregates having a β-sheet structure is related to the onset of neurodegenerative diseases such as Parkinson's and Alzheimer's[12]; moreover, these aggregates have recently been used as a highly biocompatible matrix for drug delivery [5,13–15].

Both the structure of BSA and the morphology of its aggregates are highly dependent on pH. While the self-assembling of the N form leads to conformationally disordered aggregates, for pH values lower than the isoelectric point (approx. 5) in which the F form prevails, the aggregates are more ordered, characterized by the beta-sheet conformation typical of amyloid species. In the present study, we follow the thermal denaturation of BSA at pH 5 at different concentrations, where both N and F isoforms are stable at room temperature[4]. Despite the numerous studies on the aggregation of this model protein, a detailed characterization of small pre-fibrillar aggregate formation from BSA F-isoform is still lacking.

Protein self-assembling is the result of a delicate balance between hydrophilic and hydrophobic interactions; in this respect, the low surface charge should emphasize the hydrophobic contribution to aggregation. To characterize these interactions is important in defining the properties of materials derived from protein aggregates or preventing the formation of amyloid species and prolonging the protein shelf-life. At pH 5 BSA shows a maximum of apparent partial specific volume, and a maximum specific adiabatic compressibility [16]. Besides, it has a surface charge equal to 9 [16,17], and SAXS measurements show that the dimeric species are stable at room temperature when the concentration is equal to 50 mg/ml; in fact, not only pH but also protein concentration play a fundamental role to define the type and strength of intermolecular interactions between native and non-native structures. While many denaturation and aggregation studies are conducted on micromolar BSA solutions, in this work we present a characterization conducted on millimolar solutions (30-60 mg/ml), to probe, together with the effect of the surface charge, that of self-crowding, closer to the natural conditions that occur for this protein[18] .We characterized the heat-induced conformational rearrangement by using IR absorption and circular dichroism (CD) from both a thermodynamic and kinetic point of view. It is known that the high temperature or the presence of additives, is able to favor the formation of aggregates, even of considerable size, within a few minutes when the concentration is high [19-21]. In the case of BSA, however, the formation of oligomers of limited size can also occur at room temperature, especially for very low pH values [22]. Many microscopic and spectroscopic techniques have been used to characterize the process leading to the formation of large supramolecular structures [22–25]. IR absorption and CD spectroscopy are two effective techniques in studying the conformational variations of proteins and their intermolecular aggregation processes; the different sensitivity they show to reveal reversible and irreversible denaturation processes makes them somewhat complementary in the characterization of the protein systems. The information one can obtain from the two techniques allows to characterize the protein structure at the molecular level (secondary and tertiary structural properties of the single polypeptide chain). Furthermore, FTIR spectroscopy allows to selectively probe the process of small species formation, thus allowing to distinguish the oligomerization from the much more extensively studied fibrillation process [21,22,26]. The conformational investigation is supported by an analysis of the kinetics data through the Maximum Entropy Method (MEM), which is a valuable tool for gathering information at the molecular level. [27]The evolution of the characteristic CD signals of the secondary structure of the protein as the temperature varies in the range between 12 and 84°C has been studied in detail [28,29]; however, the high protein concentration, close to the physiological value of tens of milligrams per milliliter, is always considered as an issue with this technique. In the present work we perform CD measurements on both low (0.2 mg/ml) and high (60 mg/ml) concentration

solutions: significant differences have been evidenced between BSA molecular structure in the two concentration regimes. Moreover, the IR marker band of intermolecular β-structures is used as a probe of the aggregation kinetics [30–34], and the mechanism of assembling at different concentrations is described. We characterize this aggregate formation using MEM to fit the kinetic curves obtained in the melting range; this allows recognizing the main steps of the first two hours of assembling. For the initial few minute reaction, we evaluated the activation energy of the aggregation rate to be compared with the one obtained for BSA fibrillation.

Materials and Methods

Samples

Bovine serum albumin (98%) and D_2O was purchased from Sigma—Aldrich and used without further purification. The solutions were prepared by dissolving a known mass of protein in a given quantity of deuterated water (pH = 5 obtained by adding HCl). Concentration comes expressed as the mass of solute per volume of water (mg/ml). Each mixture has been sonicated to ensure complete solubility of the solute and homogeneity of the solution.

Circular Dichroism

Circular dichroism measurements were performed using the Jasco J810 spectropolarimeter. Each spectrum was collected in the range from 220 to 350 nm, with a scan speed of 50 nm/min. Quartz cuvettes with path-length of 1 mm, and 0.01 mm were used, to obtain the optimum signal-to-noise ratio for the BSA samples with concentrations of 0.2 mg/ml – 3 μM and the 60 mg/ml - 900 μM, respectively. Temperature was controlled through a thermal bath, with steps of 3 °C, and equilibration time of 3 min. The exact protein concentration was checked by means of a Jasco V-570 Spectrophotometer, using the extinction coefficient of BSA at 280 nm.[35] The temperature evolution of CD spectra was monitored on the variation of intensity at 222 nm with respect to the profile measured at 12°C, thus evaluating the relative ellipticity ($\theta_{\underline{\lambda}} rel$) in the 12-84°C range.

FTIR

Infrared absorption measurements were carried out using a Bruker Tensor 27 FTIR spectrometer (Ettlingen, Germany) with a resolution of 1 cm^{-1} in the 5000-900 cm^{-1} range. For FTIR measurements, 10 µl of protein solution was sandwiched between two calcium fluoride windows. The temperature was controlled using an FTIR600 Infrared Stage (Linkam Scientific Instruments, Tadworth, Surrey, UK). The temperature dependence of the FTIR spectra was studied by cooling the sample from room temperature down to a minimum of 12°C at a rate of approximately 1°C min^{-1}; the sample was thermally equilibrated at 12°C for 30 min and subsequently heated up at a rate of 1°C min^{-1}. The 12-84°C temperature range was explored by measuring one spectrum every 2°C with a step-scan routine: 120 s heating and 120 s thermalization to record the FTIR spectrum at a fixed temperature. The time dependence of the Amide I band was also monitored at a fixed temperature in the 60-75°C range, by recording the FTIR spectrum every 60 s for two hours.

Maximum Entropy method

The kinetics of aggregate formation have been fitted by the function (1) and the Maximum Entropy method using the MemExp Software[36]. MEM entails the maximization of the function Q defined in eq (4):

$$Q = S - \lambda\chi^2 - \alpha I \qquad (4)$$

where S is the information entropy, I is a normalization factor, and λ and α are Lagrange multipliers. In the definition of χ^2, the standard errors in the measured data were assumed to be Gaussian type. The choice of the best-fit function was made by considering the magnitude of χ^2 and of the correlation length of the residuals. MEM has revealed a powerful tool for analyzing kinetics and gaining insights into the conformational distributions and the micro-heterogeneity of different samples[37,38].

Results and discussion

In Fig. 1 the CD profiles of a dilute (0.2 mg/ml - 3μM) and a concentrated (60 mg/ml - 900 μM) BSA solutions are shown in the region of π–π* and n–π* transitions of amidic groups: some differences are evidenced both at the lowest (12°C) and the highest (84°C) temperatures between spectra of these two samples.

The 208-222 nm double minimum in the low temperature spectra suggests that the dominating conformation of BSA in the diluted sample is α-helix.[35,39] As the temperature increases, the profile of the double minimum becomes broader and broader and the relative intensity of the two components is altered to such an extent that they cannot be distinguished anymore, thus signaling the protein unfolding. Quite interestingly, in the more concentrated sample the 208 nm minimum at T=12°C is much reduced with respect to the 222 nm component, a feature that is related to the instability observed by Baler et al. [8]: on increasing the BSA concentration a smaller helix fraction is expected due to protein-protein interactions and to solvent exposure of the side chains. The temperature evolution of helical structures can be followed on the CD intensity at 222 nm, as shown in Fig. 1 (panels c,d); these curves easily allow recognizing the melting range in the region where the negative peak of ($\delta\theta_{\underline{\lambda}}rel/\delta$T) is observed.

However, the description of the unfolding process in both dilute and concentrated solutions can be inspected by BestSel deconvolution analysis[40] to reproduce, in a selective manner, the different components of BSA secondary structure as a function of temperature (see Fig.2).

At room temperature, we obtain an estimate of 52% helix content for the dilute BSA solution, in very good agreement with MD simulation results, estimated for both N and F isoforms .[8] Our deconvolution results of 0.2 mg/ml solution suggest that the average melting temperature is observed at about 55°C (Fig.2b) with most helices converted into unordered arrangements, and a simultaneous increase of β structures. Besides, a two-state van't Hoff model allows to reproduce the increase (decrease) of unordered (ordered) structures and determine an average enthalpy change of about 100 kJ mol^{-1}, in agreement with recent data of Precupas et al. .[41]

The wide temperature melting range observed in our measurements, is related to the various structural changes of BSA[3,30]: as a result of the different thermal stability of the three protein domains, the melting range of dilute solution extends from 35° to 65°C.

The conformation of BSA changes significantly at 60 mg/ml concentration; also in this case we describe the rearrangement of secondary structure in the whole 12-84°C temperature range. The data shown in Fig. 3 evidence that the helix fraction for the concentrated solution is lower even at room temperature, and this is in favor of a larger fraction of antiparallel β-strands; at T>60°C the fraction of α-helix is less than 10%.

The melting temperature observed for this sample is roughly the same as for the dilute case, while the melting range is much narrower. On the other hand, the melting enthalpy turns out to be much higher (500 kJ mol^{-1} ca.) than what was found for the low concentration system. Although the estimate was performed in a different regime (micromolar), our results follow the same trend as those obtained by DSC measurements [42]: the melting enthalpy increases with concentration. In the high concentration regime, the less stable domain III unfolds at lower temperatures which explains the lower helix fraction obtained for the 60 mg/ml solution, and the higher transition enthalpy as due to the unfolding of the more stable domains. This indicates the N⇄F equilibrium to be shifted toward the F isoform at room temperature, thus favoring the formation of ordered aggregates on increasing temperature. In fact, in the 50-65°C range the fraction of helices shows a rapid decrease, while that of β-strands shows a rapid increase: this latter is related to the ordered aggregation of BSA to give supramolecular oligomeric β-structures. Fig. 3 also shows a constant increase of unordered structures upon the entire thermal path from 12 to 84°C.

To monitor the ordered aggregation, we followed the heating process of the concentrated solution by FTIR absorption spectroscopy. Two characteristic absorptions at 1618 and 1690 cm^{-1} ca. are assigned to the Amide I band (AmI) of intermolecular antisymmetric β-structures and act as selective probes of the pre-fibrillar aggregation[43]. Besides, due to isotopic substitution on NH groups of amidic functionalities, the open structure of the polypeptide chain can be efficiently monitored by the intensity of the 1540 cm^{-1} band, which is expected to be proportional to the concentration of amide groups that are not solvent exposed. H/D complete exchange on NH groups causes the Amide II band, assigned to N-H(D) in-plane bending motion, to shift to 1450 cm^{-1}, and the intensity at 1540 cm^{-1} ca. to be completely vanishing (see spectral profile in the green rectangle of the figure below): except for some oscillating noise, no signal is revealed in the 1530-1550 cm^{-1} range, even at low temperatures.

In Figure 4b the position of AmI (ν_{AmI}) is shown. The AmI band results from the contributions of different secondary structures of polypeptide chains, with three components in the ranges 1615-1630 cm^{-1}, 1650-1655 $cm^{-1,}$ and 1670-1690 cm^{-1} from the inter- and intra-molecular β-sheet, the α-helix, and the turns and loops conformations, respectively. In this context, the slight increase of ν_{AmI} in the 12-50°C range is reasonably due to the loss of helices in favor of disordered conformations; at T>50°C the lower values of this parameter on increasing temperature are due to the increase of β structures. The conformational changes suggested by the frequency shift of ν_{AmI} are in excellent agreement with the results from CD spectroscopy shown in Fig.3.

In Fig. 4c the integrated intensity of the 1618 cm^{-1} shoulder (I_{agg}) is plotted against temperature. The growth of supramolecular ordered species as inspected by this feature is detected for T>58°C. This latter seems to be a critical

value for the high concentration BSA solutions. In fact, at the same temperature and pH=7.45, Dmitriev et al. observed a crossover from reversible (unfolding) to irreversible (aggregation) phase transition for a 100 mg/ml solution, leading to gelation at T>70°C.[44]

By monitoring I_{agg} we also followed the kinetics of BSA self-assembling at T≥60°C for the 60 mg/ml and 30 mg/ml BSA solutions: data are shown in Fig. 5. The log-log plot is to evidence that no lag-time was revealed at any experimental temperature and that the concave profile of I_{agg} vs. time is in accord with a downhill polymerization as observed for this protein at different pH and concentration conditions .[45,46]

According to this type of polymerization, the rate-limiting step of the process is not the formation of a nucleus having a critical size; it is rather the conformational rearrangement of the monomer or oligomers to give a structure P* that is prone to aggregation.[47] As suggested by the name, the model considers that the transition to these activated species P* is energetically favored (no lag time is observed) and has a weak concentration dependence: our data agree with these assumptions. Moreover, we do not observe any increase of intensity at 1618 cm^{-1} by monitoring the AmI profile at 58°C for two hours: this could probably suggest that P* corresponds to the state where the BSA chain has the largest fraction of β-structures (see Fig. 3), or/and that an extremely low aggregation rate is observed at this temperature. The first of these two hypotheses was also proposed for BSA aggregation at physiologic conditions and lower concentrations[7]. On the other hand, the situation is completely different from what we observed for lysozyme under denaturing conditions: in that case, we noticed the appearance of ordered aggregates as soon as unfolded species were formed and evidenced the participation of native structures to the aggregation process[32]. A further difference is recognized with respect to lysozyme self-assembling: the aggregate band is more and more intense on increasing temperature. On the contrary, we observed that the thermal stability of lysozyme oligomers has a maximum at about 65°C [30,32].

Fig. 5 evidences that, within one hour from the beginning of the reaction, a different plateau is reached at different temperatures (I_{final}), both for the 30 and 60 mg/ml solutions. The temperature dependence of this limit concentration is shown in Fig. 6a: it resembles the trend reported in Fig. 4c.

We incubated the 60 mg/ml solution at 75°C for 1 h and obtained the transparent gel shown in Fig.6b, which is indicative of the presence of rather small aggregate dimensions and a homogeneous distribution of species.

To glean insights on the complex mechanism of aggregate formation in the entire explored time range, we reproduced the curves of Fig. 5 by using the Maximum Entropy Method and the following formula:

$$A = \sum_{i=1}^{N} A_{0i}(1 - e^{-k_i t}) \qquad (1)$$

In equation (1), A is the absorbance value at 1618 cm^{-1}, which grows in time as a sum of N exponential functions, each characterized by a specific kinetic constant, k_i, and an initial spectral contribution, A_{0i}. The outputs of the fitting procedure through the Maximum Entropy Method (see the Materials and Methods section for more details) are reported in Figure 7 for both the 30 (on the left) and the 60 (on the right) mg/ml BSA solutions.

It is evident that in every case, there is a broad distribution of species and hence of kinetic constants' values. The percentage weight for each contribution is estimated through the following equation:

$$\%weight_i = \frac{A_{0i}}{\sum_{i=1}^{N} A_{0i}} * 100 \qquad (2)$$

In the case of the 30 mg/ml sample at 60°C, BSA shows a broad distribution of kinetic constants included between 0.01 and 1 min^{-1}, and with a maximum at 0.102 min^{-1}; at higher temperatures, the distribution shrinks. This evidence is quantitatively proved by the values of the Fuzzy Entropy, H, reported in Table 1. The Fuzzy Entropy for any sample of conformers is given by the following equation [48]:

$$H = -\frac{1}{log(N)} \sum_{i=1}^{N} (w_i log(w_i)) \qquad (3)$$

In equation (3), $w_i = \frac{\%weight_i}{100}$. H, as defined in equation 3, is normalized and can assume values included between 0 and 1. The broader the distribution of conformers, the larger the value of H[49,50]. For the 30 mg/ml solution, H=0.92 at 60°C, and it decreases at higher temperatures. At 62 °C, there are two distinct groups of conformers , whose k_i values are peaked at 0.268 min^{-1} and 0.053 min^{-1}, respectively. At the three other temperatures, the distributions show just one maximum that shifts from 0.409 min^{-1} (at 65°C) to 0.442 min^{-1} (at 68°C), up to 0.602 min^{-1} (at 75°C); a shoulder is present on the low k_i-value side. The reduced distribution of the aggregation kinetics on increasing temperature is quantified by the small H value (=0.69) of 30 mg/ml solution at 75°C; at 60 mg/ml BSA concentration, a minimum H value (=0.70) is obtained at 70°C.

In the case of the concentrated sample, the distribution of conformers always appears as constituted by two families: one for large values of the kinetic constants and responsible for the initial parts of the process, and the other for smaller values of the k_i, which is responsible for the slower parts of the kinetics. The fastest conformers of the concentrated solution have kinetic constants that are always larger than those characterizing the 30 mg/ml sample counterpart. In other words, the higher concentration catalyzes the conformational rearrangement, which is the rate-determining step of the aggregation process.

The detailed analysis of temperature dependence of the initial aggregation rate was evaluated from the initial slope of curves reported in Fig.5; the Arrhenius plot of this rate v_0 is shown in Fig.8.

The Arrhenius plot of v_0 allows estimating a 108±20 kJ mol^{-1} activation energy for the aggregation process observed at 60 mg/ml; except at the lowest temperature, the same energy is also assessed for the 30 mg/ml solution. A similar value was obtained by Bhattacharya et al.[45] for BSA fibrillation and this is a confirmation that the formation of small and large aggregates has the same energetics, as suggested by the downhill polymerization. By comparison of our data with those reported in the literature, one can notice the absence of a lag phase for both small and large ordered aggregate formation, at acidic and physiologic conditions, in the 5-60 mg/ml range :[51] this is a further confirmation that, under this wide range of experimental conditions, the aggregation kinetics follows the same mechanism. It is worth noting that, since the activation energy is the same irrespective of protein concentration, the catalytic effects observed with the Maximum Entropy Method could have an entropic origin. As observed with CD measurements, at 60 mg/ml the protein is more prone to favor the conformational transition leading to ordered oligomers: this could be related to a higher activation entropy rather than a lower energy cost.

Conclusions

Fibrillar or pre-fibrillar species giving rise to amyloid fibers, and smartly replicated in vitro from a wide number of proteins, besides being notorious for their involvement with neurodegenerative disorders, are discovered to be also a benchmark as drug carriers for new biotechnological and medical applications. This makes them a multifaceted and always challenging research topic. Among the multitude of proteins, BSA is discovered to be a very suitable model for studying the physico-chemical features of the *fibril-like* supramolecular structures, thanks to its large availability and tendency to aggregate and to gel under acidic conditions.

In the present work, CD analysis performed on a millimolar BSA solution (60 mg/ml) evidenced different stability of the protein subunits (domains) and different conformational rearrangement with respect to the solution at micromolar concentration (0.2 mg/ml), which is by far the regime usually explored to follow the changes of the secondary structure[28,29]. The different stability of BSA subdomains has a strong impact on the extent and type of protein aggregation and our conformational analysis suggests that at room temperature the F isoform prevails over the N structure which is stable in the low concentration regime.

The combined use of FTIR and CD techniques allowed us to follow, on a molecular scale, the heat-induced BSA aggregation, at pH=5, over the 12-84°C temperature range. We evidenced that aggregation occurs at T>58°C, at the

unfolding of the helical structure. This confirms the exposure of hydrophobic regions to the solvent as the initiation step of the self-assembling process. However, differently to what was observed at lower concentrations[6], aggregation led to ordered β-structures which usually require a change of both tertiary and secondary structure. Thanks to the possibility to perform CD and FTIR measurements in the same experimental conditions, we were able to identify the aggregation-prone species at the unfolding of the F isoform and to confirm the process as a downhill polymerization. In fact, no lag-time and weak concentration dependence were observed in the self-assembling reaction. The Maximum Entropy Method, applied for fitting the kinetic curves, has then provided the distribution of kinetic constants of the hierarchical aggregation path, within two hours reaction. One or two distributions of kinetic constants (depending on temperature and concentration) were recognized for the process. We derived the activation energy of the initial self-assembling step leading to the formation of small/intermediate aggregates, observing that the growth of both small and large species is controlled by the same interactions, in agreement with the nature of the downhill polymerization. The methods of investigation here adopted could be favorably extended to study character and typology of aggregation processes of human proteins under different environmental conditions.

References

[1] K. Murayama, M. Tomida, Heat-induced secondary structure and conformation change of bovine serum albumin investigated by Fourier transform infrared spectroscopy, Biochemistry. 43 (2004) 11526–11532.

[2] Y. Li, J. Lee, J. Lal, L. An, Q. Huang, Effects of pH on the interactions and conformation of bovine serum albumin: comparison between chemical force microscopy and small-angle neutron scattering, J. Phys. Chem. B. 112 (2008) 3797–3806.

[3] M. Dockal, D.C. Carter, F. Rüker, Conformational transitions of the three recombinant domains of human serum albumin depending on pH, J. Biol. Chem. 275 (2000) 3042–3050.

[4] X. Zhou, Z. He, H. Huang, Secondary structure transitions of Bovine serum albumin induced by temperature variation, Vib. Spectrosc. 92 (2017) 273–279.

[5] G. Navarra, C. Peres, M. Contardi, P. Picone, P.L. San Biagio, M. Di Carlo, D. Giacomazza, V. Militello, Heat- and pH-induced BSA conformational changes, hydrogel formation and application as 3D cell scaffold, Arch. Biochem. Biophys. 606 (2016) 134–142.

[6] V. Vetri, F. Librizzi, M. Leone, V. Militello, Thermal aggregation of bovine serum albumin at different pH: comparison with human serum albumin, Eur. Biophys. J. 36 (2007) 717–725.

[7] D. Molodenskiy, E. Shirshin, T. Tikhonova, A. Gruzinov, G. Peters, F. Spinozzi, Thermally induced conformational changes and protein--protein interactions of bovine serum albumin in aqueous solution under different pH and ionic strengths as revealed by SAXS measurements, Phys. Chem. Chem. Phys. 19 (2017) 17143–17155.

[8] K. Baler, O.A. Martin, M.A. Carignano, G.A. Ameer, J.A. Vila, I. Szleifer, Electrostatic unfolding and interactions of albumin driven by pH changes: a molecular dynamics study, J. Phys. Chem. B. 118 (2014) 921–930.

[9] E. Edri, O. Regev, pH effects on BSA-dispersed carbon nanotubes studied by spectroscopy-enhanced composition evaluation techniques, Anal. Chem. 80 (2008) 4049–4054.

[10] J.F. Foster, SOME ASPECTS OF THE STRUCTURE AND CONFORMATIONAL PROPERTIES OF SERUM ALBUMIN, Albumin: Structure, Function and Uses. (1977) 53–84. https://doi.org/10.1016/b978-0-08-019603-9.50010-7.

[11] K. Baler, R. Michael, I. Szleifer, G.A. Ameer, Albumin Hydrogels Formed by Electrostatically Triggered Self-Assembly and Their Drug Delivery Capability, Biomacromolecules. 15 (2014) 3625–3633. https://doi.org/10.1021/bm500883h.

[12] F. Chiti, C.M. Dobson, Protein misfolding, functional amyloid, and human disease, Annu. Rev. Biochem. 75 (2006) 333–366.

[13] S. Zhang, Fabrication of novel biomaterials through molecular self-assembly, Nat. Biotechnol. 21 (2003) 1171–1178.

[14] N.A. Peppas, J.Z. Hilt, A. Khademhosseini, Hydrogels in biology and medicine: from molecular principles to bionanotechnology, Advanced. (2006). https://onlinelibrary.wiley.com/doi/abs/10.1002/adma.200501612.

[15] B.V. Slaughter, S.S. Khurshid, O.Z. Fisher, A. Khademhosseini, N.A. Peppas, Hydrogels in regenerative medicine, Adv. Mater. 21 (2009) 3307–3329.

[16] N.E. Kadi, N. El Kadi, N. Taulier, J.Y. Le Huérou, M. Gindre, W. Urbach, I. Nwigwe, P.C. Kahn, M. Waks, Unfolding and Refolding of Bovine Serum Albumin at Acid pH: Ultrasound and Structural Studies, Biophysical Journal. 91 (2006) 3397–3404. https://doi.org/10.1529/biophysj.106.088963.

[17] L.R.S. Barbosa, M.G. Ortore, F. Spinozzi, P. Mariani, S. Bernstorff, R. Itri, The importance of protein-protein interactions on the pH-induced conformational changes of bovine serum albumin: a small-angle X-ray scattering study, Biophys. J. 98 (2010) 147–157.

[18] S. Biswas, S.K. Mukherjee, H. Lal, S. Karmakar, P.K. Chowdhury, pH dependent domain dynamics of HSA controlled by protein based crowding agents, Chemical Physics Letters. 688 (2017) 98–105. https://doi.org/10.1016/j.cplett.2017.09.034.

[19] K. Murayama, M. Tomida, Heat-Induced Secondary Structure and Conformation Change of Bovine Serum Albumin Investigated by Fourier Transform Infrared Spectroscopy, Biochemistry. 43 (2004) 11526–11532. https://doi.org/10.1021/bi0489154.

[20] M. Dasgupta, N. Kishore, Selective inhibition of aggregation/fibrillation of bovine serum albumin by osmolytes: Mechanistic and energetics insights, PLoS One. 12 (2017) e0172208.

[21] N.A. Al-Shabib, J.M. Khan, M.A. Alsenaidy, A.M. Alsenaidy, M.S. Khan, F.M. Husain, M.R. Khan, M. Naseem, P. Sen, P. Alam, R.H. Khan, Unveiling the stimulatory effects of tartrazine on human and bovine serum albumin fibrillogenesis: Spectroscopic and microscopic study, Spectrochim. Acta A Mol. Biomol. Spectrosc. 191 (2018) 116–124.

[22] J.J. Babcock, L. Brancaleon, Bovine serum albumin oligomers in the E- and B-forms at low protein concentration and ionic strength, Int. J. Biol. Macromol. 53 (2013) 42–53.

[23] S. Bondos, Methods for Measuring Protein Aggregation, Current Analytical Chemistry. 2 (2006) 157–170.

https://doi.org/10.2174/157341106776359140.
[24] R.M. Murphy, C.C. Lee, Laser Light Scattering as an Indispensable Tool for Probing Protein Aggregation, Misbehaving Proteins. (n.d.) 147–165. https://doi.org/10.1007/978-0-387-36063-8_7.
[25] M.E.M. Cromwell, C. Felten, H. Flores, J. Liu, S.J. Shire, Self-Association of Therapeutic Proteins, Misbehaving Proteins. (n.d.) 313–330. https://doi.org/10.1007/978-0-387-36063-8_14.
[26] R. Ghosh, N. Kishore, Physicochemical Insights into the Role of Drug Functionality in Fibrillation Inhibition of Bovine Serum Albumin, The Journal of Physical Chemistry B. 124 (2020) 8989–9008. https://doi.org/10.1021/acs.jpcb.0c06167.
[27] J.C. Brochon, Maximum entropy method of data analysis in time-resolved spectroscopy, Methods Enzymol. 240 (1994) 262–311.
[28] A. Michnik, K. Michalik, Z. Drzazga, Stability of bovine serum albumin at different pH, J. Therm. Anal. Calorim. 80 (2005) 399–406.
[29] S. Kundu, C. Banerjee, N. Sarkar, Inhibiting the Fibrillation of Serum Albumin Proteins in the Presence of Surface Active Ionic Liquids (SAILs) at Low pH: Spectroscopic and Microscopic Study, J. Phys. Chem. B. 121 (2017) 7550–7560.
[30] A. Giugliarelli, M. Paolantoni, A. Morresi, P. Sassi, Denaturation and preservation of globular proteins: the role of DMSO, J. Phys. Chem. B. 116 (2012) 13361–13367.
[31] A. Giugliarelli, P. Sassi, M. Paolantoni, A. Morresi, R. Dukor, L. Nafie, Vibrational circular dichroism spectra of lysozyme solutions: solvent effects on thermal denaturation processes, J. Phys. Chem. B. 117 (2013) 2645–2652.
[32] P. Sassi, A. Giugliarelli, M. Paolantoni, A. Morresi, G. Onori, Unfolding and aggregation of lysozyme: a thermodynamic and kinetic study by FTIR spectroscopy, Biophys. Chem. 158 (2011) 46–53.
[33] A. Giugliarelli, L. Tarpani, L. Latterini, A. Morresi, M. Paolantoni, P. Sassi, Spectroscopic and Microscopic Studies of Aggregation and Fibrillation of Lysozyme in Water/Ethanol Solutions, J. Phys. Chem. B. 119 (2015) 13009–13017.
[34] M. Barbalinardo, A. Antosova, M. Gambucci, Z. Bednarikova, C. Albonetti, F. Valle, P. Sassi, L. Latterini, Z. Gazova, E. Bystrenova, Effect of metallic nanoparticles on amyloid fibrils and their influence to neural cell toxicity, Nano Res. 13 (2020) 1081–1089.
[35] S.M. Kelly, T.J. Jess, N.C. Price, How to study proteins by circular dichroism, Biochim. Biophys. Acta. 1751 (2005) 119–139.
[36] P.J. Steinbach, R. Ionescu, C.R. Matthews, Analysis of kinetics using a hybrid maximum-entropy/nonlinear-least-squares method: application to protein folding, Biophys. J. 82 (2002) 2244–2255.
[37] P.L. Gentili, C. Clementi, A. Romani, Ultraviolet–Visible Absorption and Luminescence Properties of Quinacridone–Barium Sulfate Solid Mixtures, Appl. Spectrosc., AS. 64 (2010) 923–929.
[38] A. Cesaretti, B. Carlotti, P.L. Gentili, C. Clementi, R. Germani, F. Elisei, Spectroscopic investigation of the pH controlled inclusion of doxycycline and oxytetracycline antibiotics in cationic micelles and their magnesium driven release, J. Phys. Chem. B. 118 (2014) 8601–8613.
[39] N.J. Greenfield, Using circular dichroism spectra to estimate protein secondary structure, Nat. Protoc. 1 (2006) 2876–2890.
[40] A. Micsonai, F. Wien, É. Bulyáki, J. Kun, É. Moussong, Y.-H. Lee, Y. Goto, M. Réfrégiers, J. Kardos, BeStSel: a web server for accurate protein secondary structure prediction and fold recognition from the circular dichroism spectra, Nucleic Acids Res. 46 (2018) W315–W322.
[41] A. Precupas, A.R. Leonties, A. Neacsu, R. Sandu, V.T. Popa, Gallic acid influence on bovine serum albumin thermal stability, New Journal of Chemistry. 43 (2019) 3891–3898. https://doi.org/10.1039/c9nj00115h.
[42] A. Michnik, K. Michalik, Z. Drzazga, Stability of bovine serum albumin at different pH, Journal of Thermal Analysis and Calorimetry. 80 (2005) 399–406. https://doi.org/10.1007/s10973-005-0667-9.
[43] J. Seo, W. Hoffmann, S. Warnke, X. Huang, S. Gewinner, W. Schöllkopf, M.T. Bowers, G. von Helden, K. Pagel, An infrared spectroscopy approach to follow β-sheet formation in peptide amyloid assemblies, Nat. Chem. 9 (2017) 39–44.
[44] A.V. Dmitriev, V.E. Vashchenkov, A.I. Fedoseev, S.G. Lushnikov, Phase transformations of bovine serum albumin: Evidences from Rayleigh-Brillouin light scattering, Journal of Raman Spectroscopy. 50 (2019) 537–547. https://doi.org/10.1002/jrs.5547.
[45] M. Bhattacharya, N. Jain, S. Mukhopadhyay, Insights into the mechanism of aggregation and fibril formation from bovine serum albumin, J. Phys. Chem. B. 115 (2011) 4195–4205.
[46] N.K. Holm, S.K. Jespersen, L.V. Thomassen, T.Y. Wolff, P. Sehgal, L.A. Thomsen, G. Christiansen, C.B. Andersen, A.D. Knudsen, D.E. Otzen, Aggregation and fibrillation of bovine serum albumin, Biochimica et Biophysica Acta (BBA) - Proteins and Proteomics. 1774 (2007) 1128–1138. https://doi.org/10.1016/j.bbapap.2007.06.008.
[47] S. Saha, S. Deep, Protein Aggregation: Elucidation of the Mechanism and Determination of Associated

Thermodynamic and Kinetic Parameters, Current Physical Chemistry. 4 (2014) 114–136. https://doi.org/10.2174/1877946803666131213233336.
[48] M. Gambucci, P.L. Gentili, P. Sassi, L. Latterini, A multi-spectroscopic approach to investigate the interactions between Gramicidin A and silver nanoparticles, Soft Matter. 15 (2019) 6571–6580.
[49] P.L. Gentili, The Fuzziness of the Molecular World and Its Perspectives, Molecules. 23 (2018) 2074.
[50] P.L. Gentili, The fuzziness of a chromogenic spirooxazine, Dyes Pigm. 110 (2014) 235–248.
[51] J. Juárez, P. Taboada, V. Mosquera, Existence of Different Structural Intermediates on the Fibrillation Pathway of Human Serum Albumin, Biophysical Journal. 96 (2009) 2353–2370. https://doi.org/10.1016/j.bpj.2008.12.3901.

Table 1. Fuzzy Entropy H for the conformers' distributions of the BSA samples.

	BSA 30 mg/mL	**BSA 60 mg/mL**
60°C	0.92±0.01	0.84±0.01
62°C	0.91±0.01	0.91±0.01
65°C	0.77±0.01	0.75±0.01
68°C	0.78±0.01	0.75±0.01
75°C	0.69±0.01	0.79±0.01

Figure captions

Figure 1. CD spectra as a function of temperature of diluted (a) and concentrated (b) BSA solutions in the region of π−π* and n−π* transitions of amide groups. Relative variation of ellipticity at 222 nm wavelength and corresponding derivative plot for dilute (c) and concentrated (d) samples.

Figure 2. (a) Curve fitting results obtained for CD spectra of a diluted BSA solution. Cyan, red and green points indicate respectively the helix, unordered and beta fractions obtained at each temperature; solid lines are the van't Hoff fitting curves. (b) The first derivative of the cyan curve is shown on panel a.

Figure 3. (a) Curve fitting results obtained for CD spectra of a concentrated BSA solution. Cyan, red and green points indicate respectively the helix, unordered and beta fractions obtained at each temperature; solid lines are the van't Hoff fitting curves. (b) The first derivative of the cyan curve is shown on panel a.

Figure 4. (a) FTIR spectra in the region of the Amide I band (BSA=30 mg/ml). Red asterisks mark the two components assigned to β-sheet intermolecular structures. (b) Wavenumber position of Amide I band maximum. (c) The integrated intensity of the 1618 cm^{-1} feature (I_{agg}) as a function of temperature.

Figure 5. Integrated intensity of 1618 cm^{-1} feature (I_{agg}) as a function of time for a 30 mg/ml (left), and a 60 mg/ml (right) solution.

Figure 6. (a) Limiting value of I_{agg} obtained for BSA solutions after two hours reaction. (b) Transparent gel obtained by heating the 60 mg/ml BSA solution at 75°C for 1 h

Figure 7. Distributions of the kinetic constants (k_i) as functions of temperature for the BSA samples at different concentrations.

Figure 8. Arrhenius plot of the initial aggregation rate v_0.

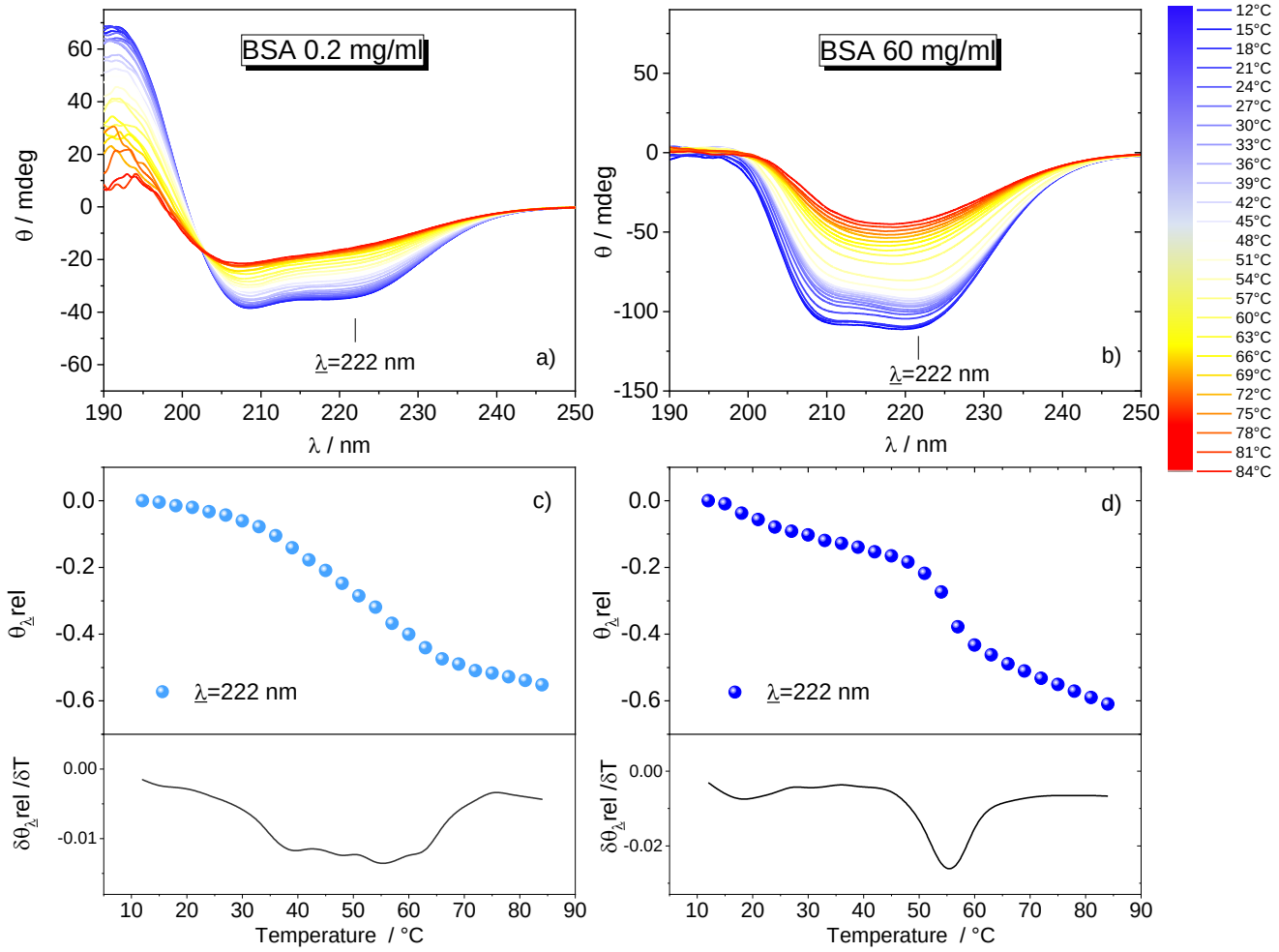
BSA 0.2 mg/ml
θ / mdeg
λ=222 nm
a)
λ / nm
BSA 60 mg/ml
b)
12°C
15°C
18°C
21°C
24°C
27°C
30°C
33°C
36°C
39°C
42°C
45°C
48°C
51°C
54°C
57°C
60°C
63°C
66°C
69°C
72°C
75°C
78°C
81°C
84°C
c)
d)
θλrel
δθλrel /δT
Temperature / °C

Figure 1

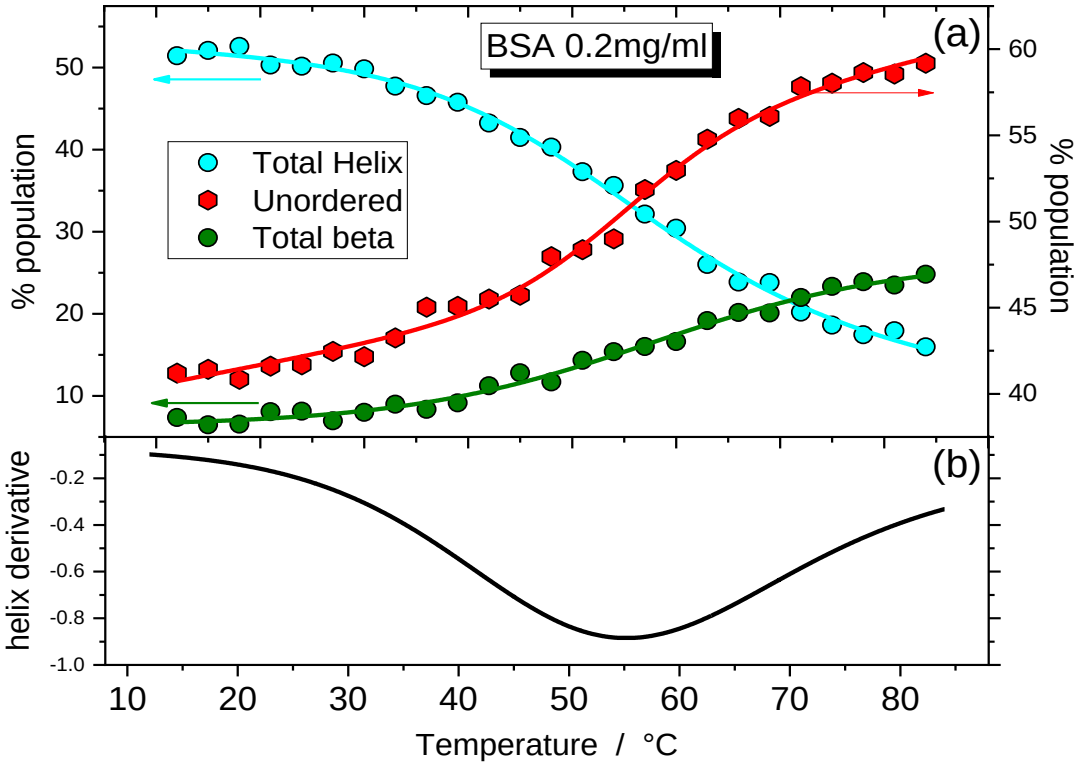
BSA 0.2mg/ml
(a)
(b)
Total Helix
Unordered
Total beta
% population
% population
helix derivative
Temperature / °C

Figure 2

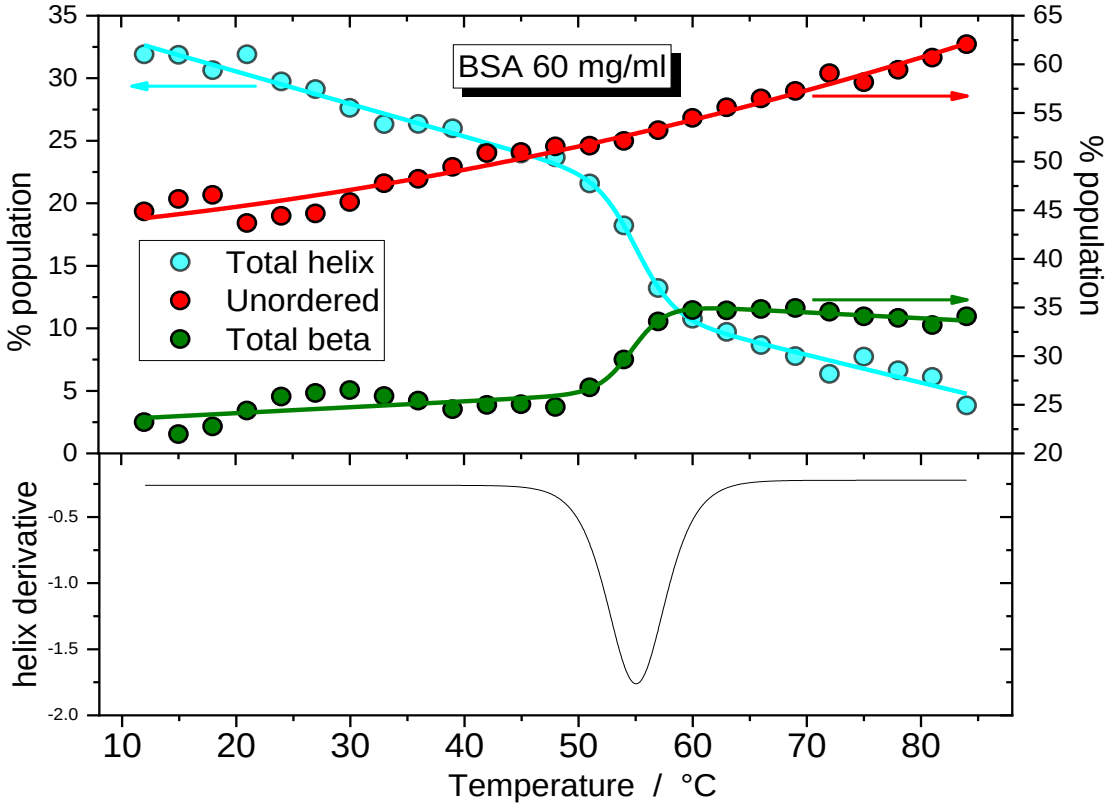
BSA 60 mg/ml
Total helix
Unordered
Total beta
% population
% population
helix derivative
Temperature / °C

Figure 3

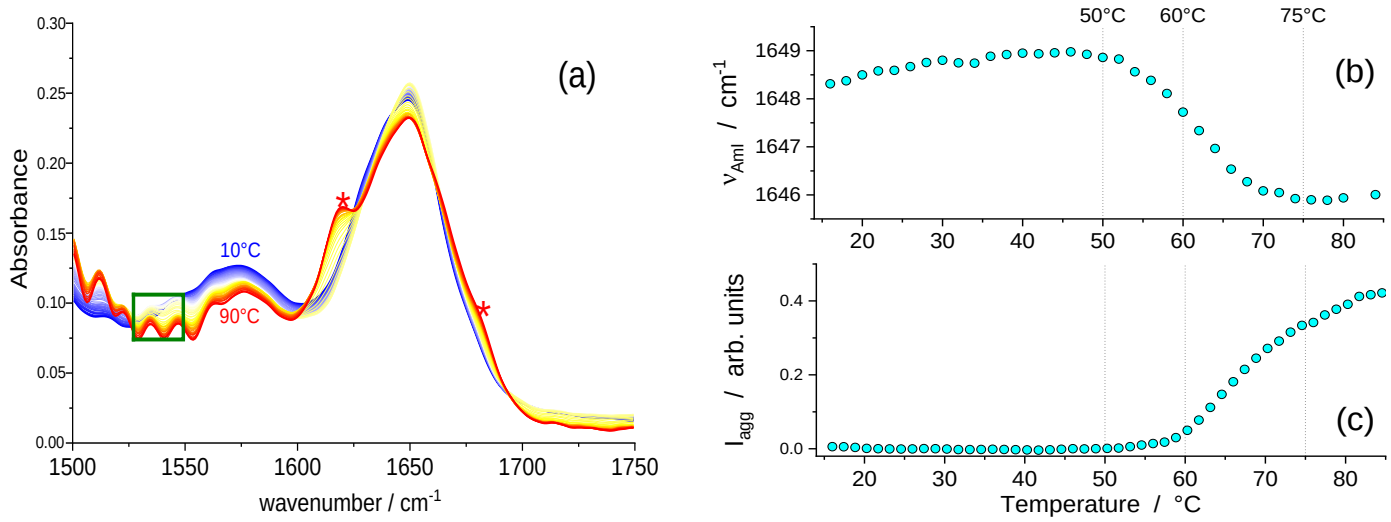
(a)
Absorbance
wavenumber / cm-1
10°C
90°C
(b)
50°C
60°C
75°C
νAmI / cm-1
(c)
Iagg / arb. units
Temperature / °C

Figure 4

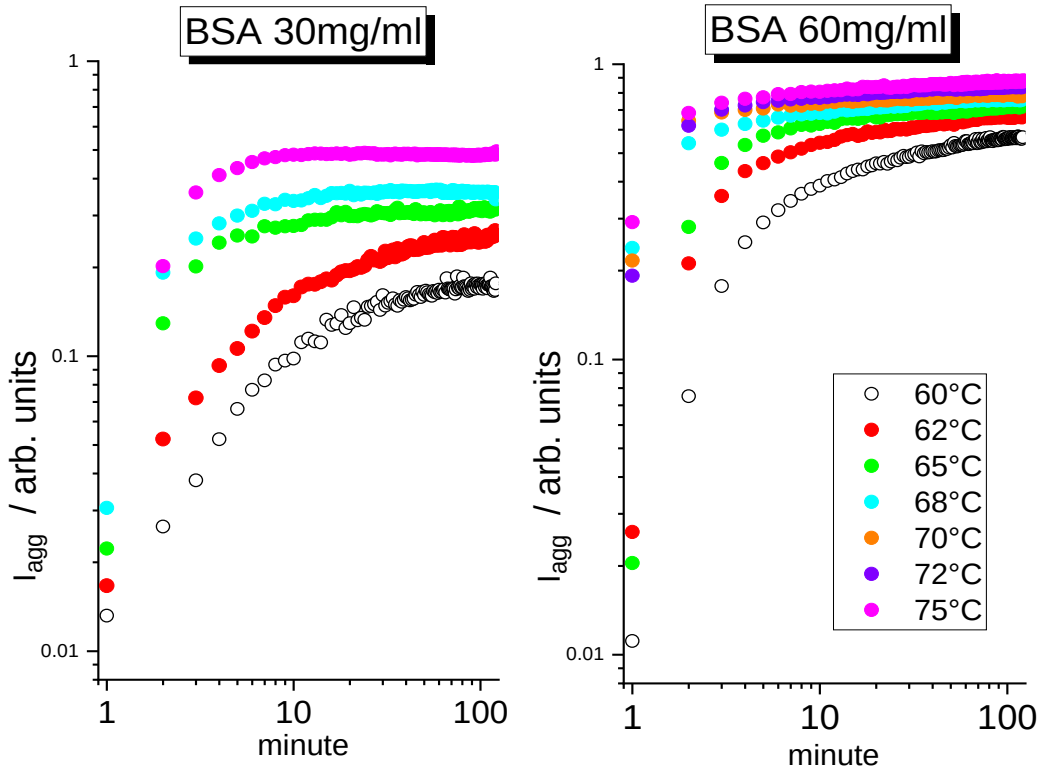
BSA 30mg/ml
BSA 60mg/ml
I_agg / arb. units
minute
1
0.1
0.01
10
100
60°C
62°C
65°C
68°C
70°C
72°C
75°C

Figure 5

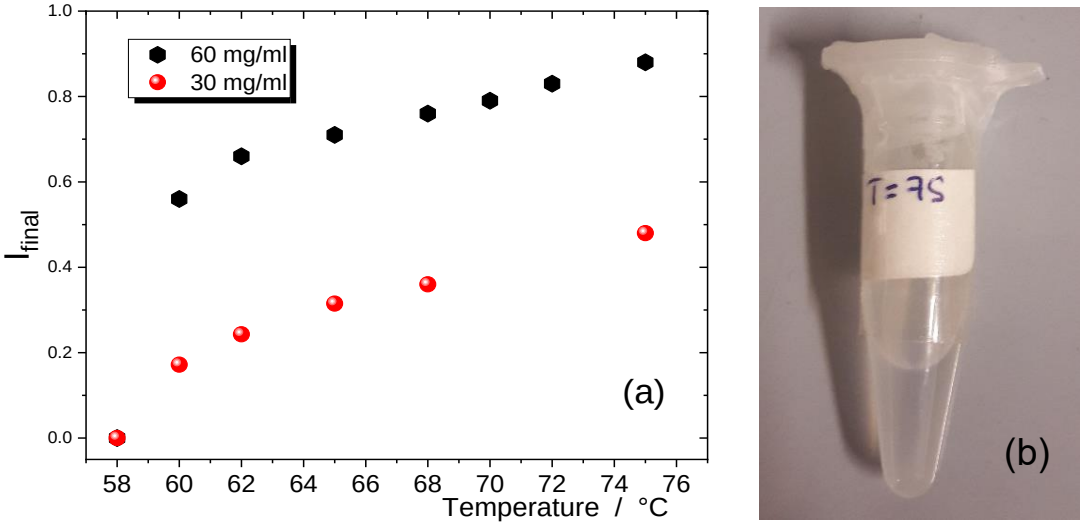
1.0
0.8
0.6
0.4
0.2
0.0
I_{final}
60 mg/ml
30 mg/ml
(a)
58
60
62
64
66
68
70
72
74
76
Temperature / °C
T=75
(b)

Figure 6

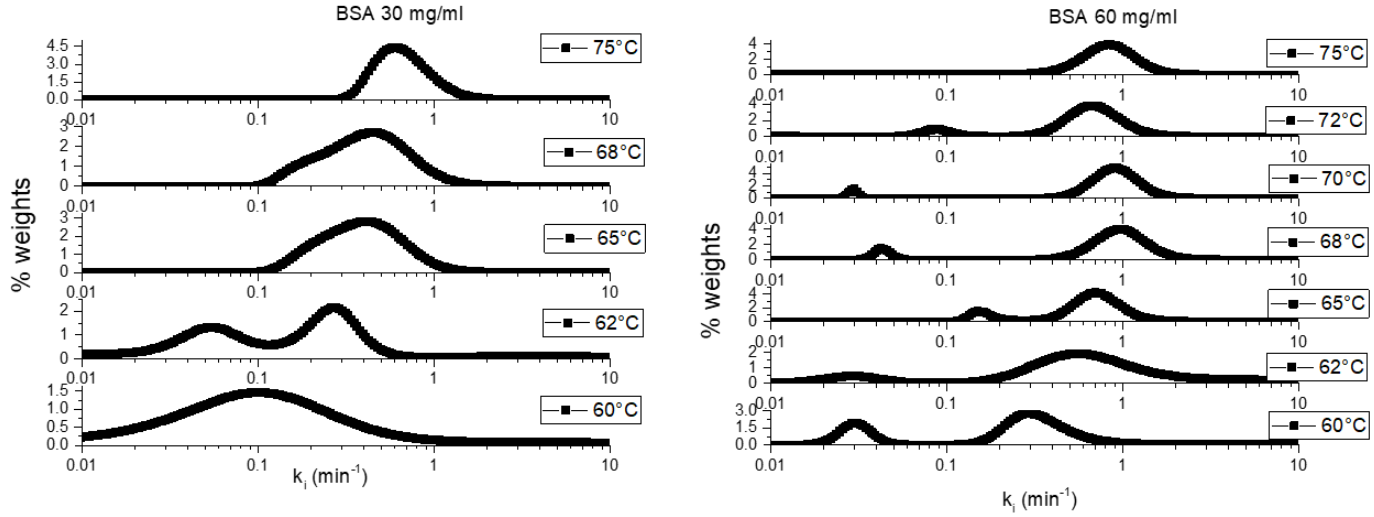
BSA 30 mg/ml
BSA 60 mg/ml
% weights
k_i (min^{-1})
75°C
72°C
70°C
68°C
65°C
62°C
60°C

Figure 7

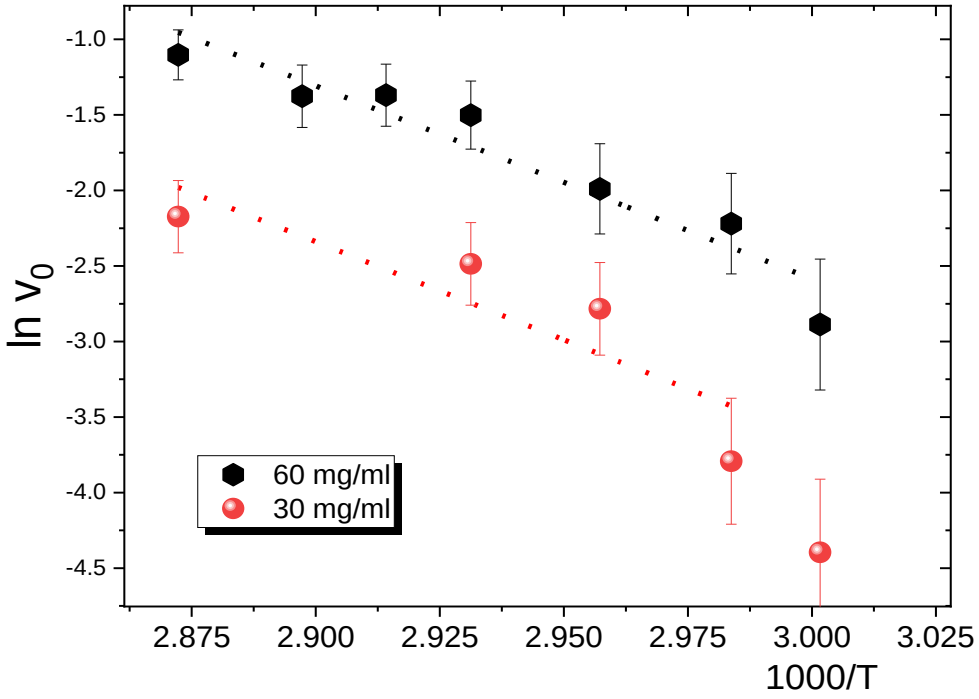
-1.0
-1.5
-2.0
-2.5
-3.0
-3.5
-4.0
-4.5
ln v_0
60 mg/ml
30 mg/ml
2.875
2.900
2.925
2.950
2.975
3.000
3.025
1000/T

Figure 8